SIAM J. APPL. MATH.
Vol. 65, No. 1, pp. 316–335

DELAYED COUPLING BETWEEN TWO NEURAL NETWORK LOOPS*

SUE ANN CAMPBELL†, R. EDWARDS‡, AND P. VAN DEN DRIESSCHE§

Abstract. Coupled loops with time delays are common in physiological systems such as neural networks. We study a Hopfield-type network that consists of a pair of one-way loops each with three neurons and two-way coupling (of either excitatory or inhibitory type) between a single neuron of each loop. Time delays are introduced in the connections between loops, and the effects of coupling strengths and delays on the network dynamics are investigated. These effects depend strongly on whether the coupling is symmetric (of the same type in both directions) or asymmetric (inhibitory in one direction and excitatory in the other). The network of six delay differential equations is studied by linear stability analysis and bifurcation theory. Loops having inherently stable zero solutions cannot be destabilized by weak coupling, regardless of the delay. Asymmetric coupling is weakly stabilizing but easily upset by delays. Symmetric coupling (if not too weak) can destabilize an inherently stable zero solution, leading to nontrivial fixed points if the gain of the neuron response function is not too negative or to oscillation otherwise. In the oscillation case, intermediate delays can restabilize the zero solution. At the borderline of the weak coupling region (symmetric or asymmetric), stability can change with delay ranges. When the coupling strengths are of the same magnitude, the oscillations of corresponding neurons in the two loops can be in phase, antiphase (symmetric coupling), or one quarter period out of phase (asymmetric coupling) depending on the delay.

Key words. neural network, coupled loops, time delay, bifurcation, oscillation

AMS subject classifications. 92B20, 34K20, 34K18, 92C20

DOI. 10.1137/S0036139903434833

1. Introduction.

Interacting loops that are capable of sustaining oscillation are common in physiological systems. One approach to modeling such systems is via coupled oscillators [13]. However, this approach does not lend itself to studying the patterns of connections between oscillators when each oscillator is itself a network. Furthermore, such networks may not be inherently oscillatory, but oscillations may arise as a result of the coupling between them. If the coupling between networks is slower than each network's internal dynamics, then additional effects can arise from the delay in the coupling. The coupling may also be faster than the internal dynamics, in which case each network could be modeled with internal delays, or both the internal connections and coupling between networks could have delays.

These questions arise in models of the brain's motor circuitry, where there are many interacting loops and feedback systems. For example, functionally separate parallel loops operate through the basal ganglia (e.g., through matrisomes in the striatum [10]) but may interact through crosstalk [2]. These loop interactions have been implicated in the generation of tremor oscillations in Parkinson's disease. The effect of the particular patterns of connections between parallel copies of a network was studied by Edwards and Gill [5], where synchrony of the network copies occurred

*Received by the editors September 16, 2003; accepted for publication (in revised form) April 22, 2004; published electronically October 28, 2004. This work was supported by the Natural Sciences and Engineering Research Council (Canada).

http://www.siam.org/journals/siap/65-1/43483.html

†Department of Applied Mathematics, University of Waterloo, Waterloo, ON N2L 3G1, Canada.

‡Centre for Nonlinear Dynamics in Physiology and Medicine, McGill University, Montréal, QC H3A 2T5, Canada (sacampbell@uwaterloo.ca).

§Department of Mathematics and Statistics, University of Victoria, Victoria, BC V8W 3P4, Canada (edwards@math.uvic.ca, pvdd@math.uvic.ca).

with appropriate crosstalk, but only when each network was in a periodic regime.

Previous work on these problems has not explicitly allowed for delays in connections. While analysis becomes more difficult with delays, their effects may be important for the applications. Research on Hopfield-type neural networks with delays, first introduced by Marcus and Westervelt [15], has shown that delays can modify dynamics in interesting ways. Delays have been inserted into various simple loop structures. Some work [14, 17, 18] has considered systems of two neurons with delayed connections. Shayer and Campbell [18] gave a detailed analysis of dynamics of two coupled units with delayed coupling and also delayed self-input, showing in particular how oscillation occurs when the interactions are strong enough, but also depending on the delays. A number of authors have studied loops of three or more neurons with delays, showing various types of behavior including oscillations, waves, steady states, and even chaos [1, 3, 7, 16, 21]. Other work has dealt with conditions for stability of steady states in Hopfield-type networks of arbitrary structure (see, for example, [4, 9, 18, 19, 20] and references therein).

The current study is an initial attempt to determine the effects of coupling (or crosstalk) between parallel copies of a network structure in the presence of delays. We focus on the simplest example that uses Hopfield network equations and in which each network copy is capable of oscillation, namely, a pair of simple loops of three neurons with one-way connections, with coupling between only one neuron of each loop. We consider the case in which the coupling between the loops, rather than the connections within the loops, is delayed. Of the previous studies mentioned above, this is perhaps most similar to that of Shayer and Campbell [18], in which the concern was also with delayed coupling between two potential oscillators, though the oscillators were single neurons with self-input rather than small loops. A single (one-way) loop of three Hopfield neurons can oscillate if their connections are inhibitory and sufficiently strong. The coupling between the loops can change this behavior, but we seek to determine how the behavior depends on the strength of coupling, the delay in coupling, and the internal gain or connection strengths within each loop.

We begin in section 2 with the dynamics of a single 3-loop (loop of three neurons with one-way connections). In section 3 we look at a pair of coupled 3-loops, giving results on stability of the trivial equilibrium and the presence of oscillation over the parameter space defined by the internal gain parameter (positive or negative) and a coupling strength parameter, allowing either inhibitory or excitatory coupling in either direction. Section 4 deals with delayed coupling between the loops. Most of the analysis is local, but where we do not have global results, numerical experiments support the conclusions. We summarize our results with a discussion (section 5).

2. Isolated 3-loop without delay. Consider a Hopfield-type network of three neurons connected in a (one-way) loop as in the following figure:

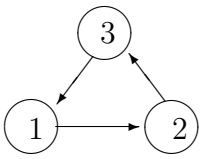

This can be described by the system of ordinary differential equations (with subscripts interpreted mod 3)

$$\frac{dx_j}{dt} = -x_j + \tanh(bx_{j-1}), \qquad j = 1, 2, 3, \tag{2.1}$$

together with initial condition $x(0) = (x_1(0), x_2(0), x_3(0))^t$. Here x_j represents the normalized voltage of neuron j and $b \in \mathbb{R}$ is the gain of the response function, assumed equal for each neuron. Interactions are inhibitory if $b < 0$ and excitatory if $b > 0$. System (2.1) always has the trivial equilibrium $(0, 0, 0)^t$, i.e., at the origin. The existence of nontrivial equilibria depends on the value of b, as in the following result.

THEOREM 2.1. *If $b > 1$, then system (2.1) has one positive symmetric and one negative symmetric equilibrium. If $b \leq 1$, then there is no nontrivial equilibrium.*

Proof. At an equilibrium of (2.1), $x_1 = \tanh(bx_3) \equiv f(x_3)$; thus $x_2 = \tanh(bx_1) = f(f(x_3))$ and $x_3 = \tanh(bx_2) = F(x_3)$, where $F(x) \equiv f(f(f(x)))$. Consider

$$h(x_3) \equiv x_3 - F(x_3) = 0. \tag{2.2}$$

Since $f'(0) = b$, $h'(0) = 1 - b^3$. Also $\lim_{x_3 \to \pm\infty} h(x_3) = \pm\infty$. From (2.2)

$$h'(x_3) = 1 - b^3 \operatorname{sech}^2(b\tanh(b\tanh(bx_3))) \operatorname{sech}^2(b\tanh(bx_3)) \operatorname{sech}^2(bx_3). \tag{2.3}$$

Thus $h'(x_3) \geq 1 - b^3$ for $b \geq 0$, which is nonnegative (for all x_3) if $b \leq 1$. Since $h(0) = 0$, there is no nontrivial equilibrium for $0 \leq b \leq 1$. For $b < 0$, (2.3) gives $h'(x_3) \geq 1$, which again shows that there is no nontrivial equilibrium.

If $b > 1$, then (2.3) gives $h''(x_3) > 0$ for all $x_3 > 0$, showing that $h(x_3)$ is concave up. This, together with $h(0) = 0$, $h'(0) < 0$, and $h(x_3) > 0$ for sufficiently large $x_3 > 0$, shows that there is a unique positive solution $x_3 = \overline{x_3} > 0$ to (2.2). The corresponding equilibrium values $\overline{x_1} > 0$, $\overline{x_2} > 0$ are determined from $\overline{x_3}$ and (2.1). Since (2.2) holds also for x_1 and x_2, it must be that $\overline{x_1} = \overline{x_2} = \overline{x_3} = \overline{x}$, giving the unique symmetric positive equilibrium as $(x_1, x_2, x_3)\,t = (\overline{x}, \overline{x}, \overline{x})^t$, with $0 < \overline{x} < 1$ from the equilibrium equation $\overline{x} = \tanh(b\overline{x})$. By symmetry, there is also a unique negative equilibrium $(x_1, x_2, x_3)\,t = (-\overline{x}, -\overline{x}, -\overline{x})^t$ if $b > 1$. ∎

The linear stability of an equilibrium $(\overline{x}, \overline{x}, \overline{x})\,t$ is governed by $\frac{dx}{dt} = Ax$, with

$$A = \begin{bmatrix} -1 & 0 & b\operatorname{sech}^2(b\overline{x}) \\ b\operatorname{sech}^2(b\overline{x}) & -1 & 0 \\ 0 & b\operatorname{sech}^2(b\overline{x}) & -1 \end{bmatrix}. \tag{2.4}$$

The following result shows that a Hopf bifurcation can occur at the trivial equilibrium.

THEOREM 2.2. *The trivial solution of (2.1) is locally asymptotically stable iff $-2 < b < 1$. At $b = -2$, the system undergoes a Hopf bifurcation and has stable limit cycle solutions for $b \lesssim -2$.*

Proof. The characteristic equation of A at $\overline{x} = 0$ in (2.4) is $-(1+\lambda)^3 + b^3 = 0$. For $-2 < b < 1$, all eigenvalues have negative real parts; thus the system is linearly stable. When $b = 1$, there is a zero eigenvalue, and for $b > 1$ there is a real positive eigenvalue. When $b = -2$, the eigenvalues are -3, $\pm\sqrt{3}i$, and for $b < -2$ there is a complex pair of eigenvalues with positive real part. At $b = -2$, matrix A is diagonalized by a matrix P of eigenvectors. Approximating $\tanh(bx_j)$ by $bx_j - b^3x_j^3/3$ (ignoring terms

of order ≥ 5) system (2.1) with $x = (x_1, x_2, x_3)^t$ is transformed by $y = P^{-1}x$ with $y = (y_1, y_2, y_3)^t$ at $b = -2$ to

$$\frac{dy}{dt} = \begin{bmatrix} 0 & -\sqrt{3} & 0 \\ \sqrt{3} & 0 & 0 \\ 0 & 0 & -3 \end{bmatrix} y + P^{-1}\left(\frac{8}{3}\right) \begin{bmatrix} (y_1 + y_3)^3 \\ \left(-y_1/2 - \sqrt{3}y_2/2 + y_3\right)^3 \\ \left(-y_1/2 + \sqrt{3}y_2/2 + y_3\right)^3 \end{bmatrix}. \tag{2.5}$$

The center manifold is given by $y_3 = H(y_1, y_2)$, with H third order because the third equation of (2.5) has no quadratic term. On the center manifold, (2.5) becomes

$$\begin{bmatrix} \frac{dy_1}{dt} \\ \frac{dy_2}{dt} \end{bmatrix} = \begin{bmatrix} 0 & -\sqrt{3} \\ \sqrt{3} & 0 \end{bmatrix} \begin{bmatrix} y_1 \\ y_2 \end{bmatrix} + \begin{bmatrix} p(y_1, y_2) \\ q(y_1, y_2) \end{bmatrix}, \tag{2.6}$$

where p and q are determined by substituting $y_3 = H(y_1, y_2)$ in the first two equations of (2.5). The standard formula for the criticality coefficient ((3.4.11) of Guckenheimer and Holmes [11]) gives $a = -1 < 0$. Since $\mathrm{Re}\,(\partial\lambda/\partial b) = -1/2$ when evaluated at $\lambda = \pm\sqrt{3}i$, $b = -2$, the supercritical Hopf bifurcation gives rise to stable periodic solutions occurring for $b \lesssim -2$. □

For a Hopfield 2-loop, the corresponding characteristic equation, $-(1+\lambda)^2 + b^2 = 0$, cannot have pure imaginary solutions. Thus a Hopfield 3-loop without delay is the smallest that can undergo a Hopf bifurcation at the origin.

Global results for the trivial equilibrium when $-2 < b \leq 1$ are now stated. Theorem 2.1 of van den Driessche and Zou [20] can be used to show easily that if $|b| < 1$, then the origin is globally asymptotically stable. For system (2.1), a Lyapunov function $V = \sum_{j=1}^{3} x_j^2$ can be used to extend the range of global stability of the origin to $-\sqrt{2} \leq b \leq 1$. Note that $b = 1$ is included here, whereas it was not in Theorem 2.2. Numerical results indicate that the full range of global stability is $-2 < b \leq 1$.

Global results for the existence and stability of periodic solutions for $b < -2$ are more difficult to obtain. However, in the limit $b \to -\infty$, when the hyperbolic tangents become step functions, the problem is easier. Glass and Pasternack [8] showed that n-dimensional networks similar to (2.1) but with step functions have globally asymptotically stable periodic solutions for $n \geq 3$. Numerical simulations of (2.1) with $b < -2$ indicate that there is a unique globally asymptotically stable periodic solution for each $b \in (-\infty, -2)$.

Consider now the stability of the nontrivial equilibria (when they exist).

THEOREM 2.3. *For $b > 1$, the positive and negative symmetric equilibria of* (2.1) *are locally asymptotically stable.*

Proof. From (2.4), the characteristic equation of A is $-(1+\lambda)^3 + b^3\,\mathrm{sech}^6(b\overline{x}) = 0$, where $(\overline{x}, \overline{x}, \overline{x})^t$ with $\overline{x} > 0$ is the positive symmetric equilibrium of (2.1) that exists for $b > 1$ (by Theorem 2.1). Thus the eigenvalues are

$$\lambda_1(\overline{x}) = -1 + b\,\mathrm{sech}^2(b\overline{x}), \quad \lambda_{2,3}(\overline{x}) = -1 - \left(\frac{1}{2} \pm i\sqrt{\frac{3}{2}}\right) b\,\mathrm{sech}^2(b\overline{x}).$$

Since $b\,\mathrm{sech}^2(b\overline{x}) > 0$, local stability follows if $\lambda_1(\overline{x}) < 0$. By (2.1), $b\overline{x} = \tanh^{-1}(\overline{x})$ and $\mathrm{sech}^2(b\overline{x}) = 1 - \overline{x}^2$, giving $\lambda_1(\overline{x}) = -1 + \tanh^{-1}(\overline{x})\left(1 - \overline{x}^2\right)/\overline{x}$ for $0 < \overline{x} < 1$, which is equivalent to $1 < b < \infty$. Also, $\lambda_1(0) = 0$ at $b = 1$. Differentiating gives

$$\frac{d\lambda_1}{d\overline{x}}(\overline{x}) = \left(\overline{x} - \left(1 + \overline{x}^2\right)\tanh^{-1}(\overline{x})\right)/\overline{x}^2,$$

which is negative, since $\tanh^{-1}(\overline{x}) > \overline{x}$. Thus $\lambda_1(\overline{x}) < 0$, showing that the positive symmetric equilibrium is locally stable. Stability for $\overline{x} < 0$ follows by symmetry. ∎

Note that $\overline{x} \to 0^+$ as $b \to 1^+$, showing that the linearly stable positive and negative equilibria bifurcate from the trivial equilibrium as it loses stability. Thus the system has a supercritical pitchfork bifurcation at $b = 1$.

3. Coupled loops without delay. Consider a pair of coupled 3-loops:

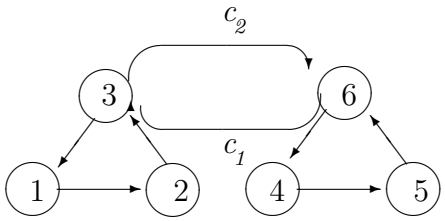

The individual loops each follow the form of (2.1). Coupling strengths are given by c_1 and c_2, where $bc_j > 0$ implies excitatory and $bc_j < 0$ implies inhibitory coupling. The system of equations for the entire system is then

$$
\begin{aligned}
&\frac{dx_1}{dt} = -x_1 + \tanh(bx_3), \quad \frac{dx_2}{dt} = -x_2 + \tanh(bx_1),\\
&\frac{dx_3}{dt} = -x_3 + \tanh(bx_2) + c_1 \tanh(bx_6),\\
&\frac{dx_4}{dt} = -x_4 + \tanh(bx_6), \quad \frac{dx_5}{dt} = -x_5 + \tanh(bx_4),\\
&\frac{dx_6}{dt} = -x_6 + \tanh(bx_5) + c_2 \tanh(bx_3),
\end{aligned}
\tag{3.1}
$$

together with initial condition $x(0) = (x_1(0), x_2(0), x_3(0), x_4(0), x_5(0), x_6(0))^t$.

Equilibria of (3.1) satisfy $x_2 = f(x_1) = f(f(x_3))$ and $x_5 = f(x_4) = f(f(x_6))$, where $f(x_j) \equiv \tanh(bx_j)$. Using the other two equations gives

$$
x_3 = F(x_3) + c_1 f(x_6), \quad x_6 = F(x_6) + c_2 f(x_3), \tag{3.2}
$$

where $F(x) = f(f(f(x)))$ as before. This can be reduced (for $c_1 \neq 0$) to

$$
g(x_3) \equiv [x_3 - F(x_3)] - c_1 f\left(f\left(f\left(\frac{1}{c_1}[x_3 - F(x_3)]\right)\right) + c_2 f(x_3)\right) = 0. \tag{3.3}
$$

Any x_3 satisfying (3.3) determines x_6 and hence all the variables at an equilibrium. Clearly the origin $x_j = 0$, $j = 1, \ldots, 6$, is an equilibrium, and our interest mostly focuses on its stability properties. However, we first show the existence of nontrivial equilibria for some b values. Define $d \equiv b^2 c_1 c_2$ and $\beta \equiv b^3$. When $d > 0$, the coupling is either excitatory or inhibitory in both directions (symmetric coupling); when $d < 0$, the coupling is excitatory in one direction and inhibitory in the other (asymmetric coupling).

THEOREM 3.1. *If $d > (1-\beta)^2$, then system* (3.1) *has nontrivial equilibria. If either* (i) $0 < \beta < 1$ *and* $d < (1-\beta)^2$, *or* (ii) $\beta < 0$ *and* $d < 1$, *then system* (3.1) *has no nontrivial equilibrium.*

Proof. Assuming $c_1 \neq 0$, differentiating (3.3) gives

$$g'(x_3) = (1 - F'(x_3))\left(1 - \beta s_1^2 s_2^2 s_3^2\right) - d s_1^2 s_4^2,$$

where s_k^2, $k = 1, \ldots, 4$, represents $\operatorname{sech}^2(\cdot)$ evaluated at some point; thus $0 < s_k^2 \leq 1$. Since $F'(0) = \beta$, it follows from the derivative above that $g'(0) = (1-\beta)^2 - d$; thus $g(x_3)$ is strictly decreasing at the origin if $d > (1-\beta)^2$. Clearly $g(0) = 0$ and $\lim_{x\to\infty} g(x_3) = \infty$ because f (and therefore F) is bounded. Thus by continuity there is at least one positive value of x_3, namely, $\overline{x}_3 > 0$, such that $g(\overline{x}_3) = 0$. By symmetry, $g(-\overline{x}_3) = 0$ and these values determine the other variables at a nontrivial equilibrium.

For $x_3 > 0$ if $\beta > 0$, then $0 < F'(x_3) < \beta$. Thus $0 < \beta < 1$ implies that $(1-\beta)^2 - d < g'(x_3)$ if $d \geq 0$, and $(1-\beta)^2 < g'(x_3) < 1 - d$ if $d \leq 0$. Thus in case (i), $g(x_3)$ is strictly increasing for all $x_3 > 0$. Similarly $\beta < 0$ implies that $\beta < F'(x_3) < 0$ and $1 - d < g'(x_3) < (1-\beta)^2$ if $d \geq 0$, and $1 < g'(x_3) < (1-\beta)^2 - d$ if $d \leq 0$. Thus in case (ii), $g(x_3)$ is strictly increasing for all $x_3 > 0$. In both cases there is no nontrivial positive equilibrium and, by symmetry, no nontrivial negative equilibrium. If $c_1 = 0$ but $c_2 \neq 0$, then reversing the roles of x_3 and x_6 leads to the same conclusions. If $c_1 = c_2 = 0$, then the results follow from Theorem 2.1. □

Note that Theorem 3.1 does not specify all regions of parameter space in which nontrivial equilibria occur. It does not provide information about the regions where β is large and positive or where β is large and negative with $d > 1$. Moreover, the number and signs of equilibria may depend on the values of c_1 and c_2 for a given d. For example, if $b = 2$ (so that $\beta = 8$) and $c_1 = c_2 = 0$, then there is one positive and one negative nontrivial equilibrium for each uncoupled loop (see Theorem 2.1) so that for the full system (3.1) there are nine equilibria, three of which have x_3 positive. However, if the coupling goes only one way, e.g., $c_1 > 0$ but $c_2 = 0$, then there can be two or four different positive equilibrium values for x_3 when $b > 1$.

The special case of symmetric coupling $c_1 = c_2$ is now considered.

THEOREM 3.2. *Let $b > 1$. If $c_1 = c_2 > 0$, then system (3.1) has a positive equilibrium $x^* = (\overline{x}_1, \overline{x}_2, \overline{x}_3, \overline{x}_1, \overline{x}_2, \overline{x}_3)^t$ and an equilibrium $-x^*$; if $c_1 = c_2 < 0$, then it has equilibria $\tilde{x}^* = (\overline{x}_1, \overline{x}_2, \overline{x}_3, -\overline{x}_1, -\overline{x}_2, -\overline{x}_3)^t$ with $\overline{x}_j > 0$, $j = 1, 2, 3$, and $-\tilde{x}^*$.*

Proof. Consider $c_1 = c_2 > 0$ and suppose that $x_3 = x_6$; then (3.2) reduces to

$$G(x_3) \equiv x_3 - F(x_3) - c_1 f(x_3) = 0$$

at an equilibrium. Note that $G(0) = 0$, $\lim_{x_3\to\infty} G(x_3) = \infty$ and $G'(0) = 1 - b^3 - c_1 b < 0$. Thus there is at least one positive zero $\overline{x}_3$ of $G(x_3)$. Since $\overline{x}_3 = \overline{x}_6 > 0$, it follows that $\overline{x}_1 = \overline{x}_4 > 0$ and $\overline{x}_2 = \overline{x}_5 > 0$. By symmetry, the negative equilibrium follows.

Consider $c_1 = c_2 < 0$ and suppose that $x_3 = -x_6$; then (3.2) reduces to

$$\tilde{G}(x_3) \equiv x_3 - F(x_3) + c_1 f(x_3) = 0$$

at an equilibrium. By the above there is at least one positive zero $\overline{x}_3$ of $\tilde{G}(x_3)$. Then $\overline{x}_1, \overline{x}_2 > 0$ and $\overline{x}_4, \overline{x}_5, \overline{x}_6 < 0$. Symmetry gives the second equilibrium. □

Numerical solutions demonstrate that additional equilibria can occur: for $c_1 = c_2 > 0$ (respectively, < 0) there may be one or three equilibria with $\overline{x}_3 > 0$, $\overline{x}_6 < 0$ (respectively, $\overline{x}_3 < 0$, $\overline{x}_6 > 0$) and an equal number of symmetric equilibria.

The linear stability of the trivial equilibrium $x_j = 0$, $j = 1, \ldots, 6$, can be determined from $\frac{dx}{dt} = Ax$ with $x = (x_1, \ldots, x_6)^t$ and

$$A = \begin{bmatrix} -1 & 0 & b & 0 & 0 & 0 \\ b & -1 & 0 & 0 & 0 & 0 \\ 0 & b & -1 & 0 & 0 & bc_1 \\ 0 & 0 & 0 & -1 & 0 & b \\ 0 & 0 & 0 & b & -1 & 0 \\ 0 & 0 & bc_2 & 0 & b & -1 \end{bmatrix}. \tag{3.4}$$

The characteristic equation for this system at $x_j = 0$ with $d \equiv b^2 c_1 c_2$ and $\beta \equiv b^3$ is

$$\left[(1+\lambda)^3 - \beta\right]^2 - d\,(1+\lambda)^4 = 0. \tag{3.5}$$

First consider the case $d \geq 0$. The characteristic equation then factors as follows:

$$\Delta_+^+(\lambda)\Delta_-^+(\lambda) \equiv \left[(1+\lambda)^3 - \beta + \sqrt{d}\,(1+\lambda)^2\right]\left[(1+\lambda)^3 - \beta - \sqrt{d}\,(1+\lambda)^2\right] = 0. \tag{3.6}$$

From the single-loop results (see Theorem 2.2), if $d = 0$, then the origin is locally asymptotically stable for $-8 < \beta < 1$ and unstable for $\beta < -8$ and $\beta > 1$. To find the stability region for $\sqrt{d} > 0$, look for curves in the βd-plane on which there is a zero or pure imaginary eigenvalue.

From (3.6), zero eigenvalues occur when $1 - \beta = \pm\sqrt{d}$. Pure imaginary eigenvalues $\lambda = i\omega$ with $\omega > 0$ make $\Delta_+^+(\lambda) = 0$ when their real and imaginary parts are zero, namely,

$$1 - 3\omega^2 - \beta + \sqrt{d}\left(1 - \omega^2\right) = 0 \quad \text{and} \quad \omega\left(3 - \omega^2 + 2\sqrt{d}\right) = 0.$$

The second condition above gives $\omega^2 = 3 + 2\sqrt{d}$, which can be substituted into the first condition to yield $\beta = -2(2 + \sqrt{d})^2$. To make $\Delta_-^+(\lambda) = 0$, there is an analogous condition where $\sqrt{d}$ is replaced by $(-\sqrt{d})$, as long as $\omega^2 = 3 - 2\sqrt{d} > 0$, i.e., $\sqrt{d} < \frac{3}{2}$, namely, $\beta = -2(2 - \sqrt{d})^2$. Note that this curve intersects the parabola of zero eigenvalues at $\beta = -\frac{1}{2}$, $d = \frac{9}{4}$. These curves are shown in Figure 3.1. It is clear by continuity from the single-loop results ($d = 0$) that the region labeled "STABLE" in the figure corresponds to linear stability of the origin. By picking points in the other regions, it can easily be checked that the origin is unstable there.

In the case where $d \leq 0$ in (3.5), factor the characteristic equation as

$$\Delta_+^-(\lambda)\Delta_-^-(\lambda) \equiv \left[(1+\lambda)^3 - \beta + i\sqrt{-d}\,(1+\lambda)^2\right]\left[(1+\lambda)^3 - \beta - i\sqrt{-d}\,(1+\lambda)^2\right] = 0. \tag{3.7}$$

Now, $\lambda = 0$ when $1 - \beta \pm i\sqrt{-d} = 0$, i.e., only at the point $\beta = 1$ and $d = 0$. Working with $\Delta_+^-(\lambda) = 0$, $\lambda = i\omega$ implies that

$$\beta = 1 - 2\sqrt{-d}\omega - 3\omega^2 \quad \text{and} \quad \sqrt{-d} = \frac{\omega\left(\omega^2 - 3\right)}{\left(1 - \omega^2\right)} \quad (\text{if } \omega^2 \neq 1), \tag{3.8}$$

giving $\beta = 1 - 3\omega^2 - 2\omega^2\left(\omega^2 - 3\right)/\left(1 - \omega^2\right)$. Working with $\Delta_-^-(\lambda) = 0$ gives this same equation in β and ω.

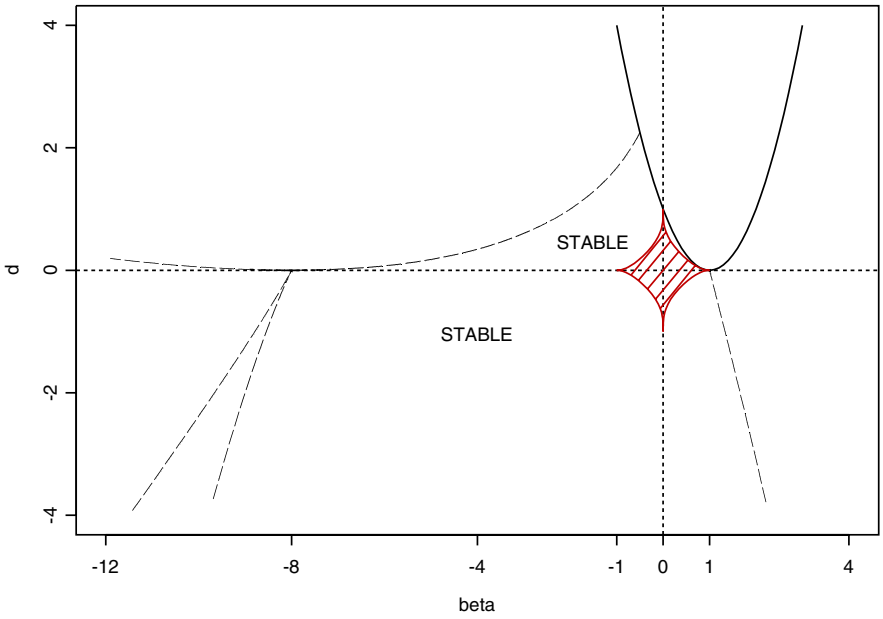

FIG. 3.1. *Regions in the parameter plane indicating stability of the origin in the coupled loop system (see* (3.1)*). The solid parabolic curve indicates parameter values where there is a zero eigenvalue. Dashed curves indicate parameter values where there are pure imaginary eigenvalues. The linearly stable regions defined by these boundaries are marked. The shaded area indicates where global stability of the origin has been proved.*

The fact that $\sqrt{-d} \geq 0$ implies that ω is in one of the intervals $\left(-\infty, -\sqrt{3}\right]$, $(-1, 0]$, or $\left(1, \sqrt{3}\right]$. In these intervals, (3.8) can be considered parametric equations for curves in the βd-plane. The curves are shown in Figure 3.1. Linear stability can again be checked by examining eigenvalues at points within each region. In the regions where $d > 0$ and $\beta > 1 - \sqrt{d}$, there are real positive eigenvalues, so the origin is an unstable node. Everywhere else outside the stability region it can be verified that there are complex conjugate pairs of eigenvalues with positive real parts, suggesting the existence of stable oscillations. Note that the pair of positive real eigenvalues becomes a complex pair with positive real part as d becomes negative $(\beta > 1)$.

For equal coupling strengths, as in the case of the single loop, global stability of the origin can be shown on a subset of the linear stability region.

THEOREM 3.3. *The origin is globally asymptotically stable for system* (3.1) *with* $|c_1| = |c_2| \equiv c > 0$ *when* $|b| < \frac{2}{\gamma}$, *where* $\gamma = 1 + 2c\,(B_1 + 1)$ *and* B_1 *is the positive root of the cubic* $8c^3 B_1\,(1 + B_1)^2 = 1$.

The proof uses the Lyapunov function $V = \sum_{j=1}^{6} a_j\, x_j^2$, where $a_j > 0$ are given as $a_1 = a_4 = \frac{B_1 + B_2}{2}$, $a_2 = a_5 = \frac{1}{4c} + \frac{B_2}{2}$, $a_3 = a_6 = \frac{1}{4c} + \frac{B_1 + 1}{2}$, and $B_2 = \sqrt{B_1/2c}$. Details of the proof are omitted. The condition $|b| < \frac{2}{\gamma}$ can be interpreted in terms of β and d by taking $d = \pm b^2 c_1^2$ (the sign depending on the sign of $c_1 c_2$, with $|c_1| = |c_2|$), and the resulting global stability region is the diamond-shaped region in Figure 3.1. Note that it covers most of the local stability region in the positive quadrant.

4. Coupled loops with delay. The case with delayed coupling connections between the 3-loops leads to the following system of delay differential equations:

$$
\begin{aligned}
&\frac{dx_1}{dt} = -x_1(t) + \tanh\left(bx_3(t)\right), \quad \frac{dx_2}{dt} = -x_2(t) + \tanh\left(bx_1(t)\right), \\
&\frac{dx_3}{dt} = -x_3(t) + \tanh\left(bx_2(t)\right) + c_1 \tanh\left(bx_6(t-\tau)\right), \\
&\frac{dx_4}{dt} = -x_4(t) + \tanh\left(bx_6(t)\right), \quad \frac{dx_5}{dt} = -x_5(t) + \tanh\left(bx_4(t)\right), \\
&\frac{dx_6}{dt} = -x_6(t) + \tanh\left(bx_5(t)\right) + c_2 \tanh\left(bx_3(t-\tau)\right),
\end{aligned} \tag{4.1}
$$

where $\tau \geq 0$ is the time delay, and when $\tau = 0$ this reduces to (3.1). To pose an initial value problem at $t = 0$, we must specify data for each variable on the interval $[-\tau, 0]$, i.e., $x_j(t) = \phi_j(t),\ -\tau \leq t \leq 0,\ j = 1, \ldots, 6$.

The equilibria for (4.1) are the same as for (3.1); in particular, Theorem 3.1 is also valid for (4.1). Using Theorem 2.1 of van den Driessche and Zou [20], we give one global stability result for system (4.1): If $|b| \max_i\{1 + |c_i|\} < 1$, then the origin is globally asymptotically stable for all values of delay $\tau \geq 0$. However, for other parameter ranges the stability of the equilibria may change due to the delay. In the next subsection we focus on the linear stability analysis of the trivial equilibrium. This then leads us to a discussion of the bifurcations of the trivial equilibrium.

4.1. Stability regions. Linearization of (4.1) about the origin gives

$$x'(t) = A_1 x(t) + A_2 x(t-\tau), \tag{4.2}$$

where

$$
A_1 = \begin{bmatrix}
-1 & 0 & b & 0 & 0 & 0 \\
b & -1 & 0 & 0 & 0 & 0 \\
0 & b & -1 & 0 & 0 & 0 \\
0 & 0 & 0 & -1 & 0 & b \\
0 & 0 & 0 & b & -1 & 0 \\
0 & 0 & 0 & 0 & b & -1
\end{bmatrix}, \quad
A_2 = \begin{bmatrix}
0 & 0 & 0 & 0 & 0 & 0 \\
0 & 0 & 0 & 0 & 0 & 0 \\
0 & 0 & 0 & 0 & 0 & bc_1 \\
0 & 0 & 0 & 0 & 0 & 0 \\
0 & 0 & 0 & 0 & 0 & 0 \\
0 & 0 & bc_2 & 0 & 0 & 0
\end{bmatrix}. \tag{4.3}
$$

The characteristic equation for this system with $d \equiv b^2 c_1 c_2$ and $\beta \equiv b^3$ is

$$\left[(1+\lambda)^3 - \beta\right]^2 - d(1+\lambda)^4 e^{-2\tau\lambda} = 0. \tag{4.4}$$

Section 3 describes the stability region of the trivial equilibrium when $\tau = 0$ (see Figure 3.1). To determine the stability region for $\tau > 0$, we determine curves in the $d\tau$-plane along which (4.4) has a zero root or a pair of pure imaginary roots. Given values of β and d for which the trivial equilibrium is stable at $\tau = 0$, it remains so for $0 \leq \tau \leq \tau_{crit}$, where τ_{crit} is the lowest value of τ on one of these curves.

First consider the case $d \geq 0$. The characteristic equation then factors as

$$
\begin{aligned}
&\Delta_+^+(\lambda)\Delta_-^+(\lambda) \\
&\quad \equiv \left[(1+\lambda)^3 - \beta + (1+\lambda)^2\sqrt{d}e^{-\tau\lambda}\right]\left[(1+\lambda)^3 - \beta - (1+\lambda)^2\sqrt{d}e^{-\tau\lambda}\right] = 0.
\end{aligned} \tag{4.5}
$$

As for the nondelayed case, zero roots occur when $d = (1-\beta)^2 \equiv d_0$.

LEMMA 4.1. *Let β and τ be fixed.*

(i) *If $\beta < 1$ and $\tau \neq 2 + \frac{3}{\beta-1}$, then $\Delta_-^+(\lambda)$ has a simple zero root when $d = d_0$; the number of roots of* (4.4) *with positive real part increases (decreases) by one as d increases through d_0 with $\tau > 2 + \frac{3}{\beta-1}$ ($\tau < 2 + \frac{3}{\beta-1}$).*

(ii) *If $\beta > 1$ and $\tau \neq 2 + \frac{3}{\beta-1}$, then $\Delta_+^+(\lambda)$ has a simple zero root when $d = d_0$; the number of roots of* (4.4) *with positive real part increases (decreases) by one as d increases through d_0 with $\tau > 2 + \frac{3}{\beta-1}$ ($\tau < 2 + \frac{3}{\beta-1}$).*

(iii) *If $\beta = 1$, both factors of* (4.5) *have a simple zero root when $d = d_0 = 0$.*

(iv) *If $\beta < 1$ ($\beta > 1$) and $\tau = 2 + \frac{3}{\beta-1}$, then $\Delta_-^+(\lambda)$ ($\Delta_+^+(\lambda)$) has a double zero root when $d = d_0$.*

Proof. The presence of zero roots follows from the facts that $\Delta_+^+(0) = 0$ when $\sqrt{d} = \beta - 1$ and $\Delta_-^+(0) = 0$ when $\sqrt{d} = 1 - \beta$. For case (iv), note that

$$\frac{d}{d\lambda}\Delta_\pm^+(\lambda) = 3(1+\lambda)^2 \pm 2(1+\lambda)\sqrt{d}e^{-\tau\lambda} \mp \tau(1+\lambda)^2\sqrt{d}e^{-\tau\lambda}.$$

Thus, if $\sqrt{d} = \pm(\beta - 1)$ and $\tau = 2 + \frac{3}{\beta-1}$, then $\frac{d}{d\lambda}\Delta_\pm^+(0) = 0$. The fact that zero is a simple root in cases (i)–(iii) also follows from this derivative.

To study the rate of change of the real part of a root, λ, of (4.5), consider either factor of this equation. For $d > 0$, differentiating with respect to d, keeping in mind that λ is a function of d, and rearranging give

$$\frac{d\lambda}{d\,d} = \frac{\pm(1+\lambda)^2\sqrt{d}e^{-\tau\lambda}}{-6d(1+\lambda)^2 \mp 4d(1+\lambda)\sqrt{d}e^{-\tau\lambda} \pm 2d\tau(1+\lambda)^2\sqrt{d}e^{-\tau\lambda}},$$

where the upper sign in $\pm$, $\mp$ refers to Δ_+^+ and the lower sign to Δ_-^+. Using (4.5) to eliminate $\pm\sqrt{d}e^{-\tau\lambda}$ and setting $\lambda = 0$ and $d = d_0$ yield

$$\left.\frac{d\lambda}{d\,d}\right|_{\lambda=0} = \frac{1}{2(\beta-1)[(\tau-2)(\beta-1)-3]}.$$

Consideration of the sign of the right-hand side completes the proofs of (i) and (ii). ∎

For $d > 0$, to find the curves where pure imaginary roots exist, set $\lambda = i\omega$ in each factor of (4.5) and separate into real and imaginary parts. Without loss of generality, take $\omega > 0$. For $\Delta_+^+(\lambda)$, isolating $\sin(\omega\tau)$ and $\cos(\omega\tau)$ yields

$$\begin{aligned} (1+\omega^2)^2\sqrt{d}\cos(\omega\tau) &= -\left((1+\omega^2)^2 - \beta(1-\omega^2)\right) \equiv -\mathcal{C}(\omega), \\ (1+\omega^2)^2\sqrt{d}\sin(\omega\tau) &= \omega\left((1+\omega^2)^2 + 2\beta\right) \equiv \mathcal{S}(\omega). \end{aligned} \tag{4.6}$$

To find d and τ in terms of β and ω, square the equations in (4.6) and add to give

$$d = d_{im}(\omega) \equiv \frac{(1+\omega^2)^3 + 2\beta(3\omega^2-1) + \beta^2}{(1+\omega^2)^2}. \tag{4.7}$$

Dividing the second equation of (4.6) by the first gives $\tan(\omega\tau) = -\mathcal{S}(\omega)/\mathcal{C}(\omega)$. However, this loses information about the signs of $\cos(\omega\tau)$ and $\sin(\omega\tau)$ that is in (4.6). Thus we introduce $y = \mathrm{Arctan}(u)$ as the branch of the arctangent function with range $(-\frac{\pi}{2}, \frac{\pi}{2})$. Note that this corresponds to $\cos(y) > 0$ and that the function

$\text{Arctan}(u) + \pi$ corresponds to $\cos(y) < 0$. The other branches of the arctangent function are obtained from these two by adding multiples of 2π. As can be seen from (4.6), the sign of $\cos(\omega\tau)$ is determined by $\mathcal{C}(\omega)$, and thus we define

$$\tau = \tau^+_{k+}(\omega) \equiv \frac{1}{\omega}\begin{cases} \text{Arctan}\left(-\frac{\mathcal{S}(\omega)}{\mathcal{C}(\omega)}\right) + 2k\pi, & \mathcal{C}(\omega) < 0, \\ \text{Arctan}\left(-\frac{\mathcal{S}(\omega)}{\mathcal{C}(\omega)}\right) + (2k+1)\pi, & \mathcal{C}(\omega) > 0, \end{cases} \tag{4.8}$$

where $k = 0, 1, \ldots$. (We do not take $k < 0$ as these branches always yield $\tau < 0$.)

In a similar manner it can be shown that the curves along which the second factor, $\Delta^+_-(\lambda)$, of (4.5) has a pair of pure imaginary roots are given by $(d, \tau) = (d_{im}(\omega), \tau^+_{k-}(\omega))$, where d_{im} is as above and

$$\tau^+_{k-}(\omega) \equiv \frac{1}{\omega}\begin{cases} \text{Arctan}\left(-\frac{\mathcal{S}(\omega)}{\mathcal{C}(\omega)}\right) + 2k\pi, & \mathcal{C}(\omega) > 0, \\ \text{Arctan}\left(-\frac{\mathcal{S}(\omega)}{\mathcal{C}(\omega)}\right) + (2k+1)\pi, & \mathcal{C}(\omega) < 0. \end{cases} \tag{4.9}$$

The zeros of $\mathcal{C}(\omega)$ define the points where the branches join. To see how the sign of $\mathcal{C}(\omega)$ varies with β and ω, rewrite the first equation of (4.6) as a quartic in ω, namely, $\mathcal{C}(\omega) = \omega^4 + (2+\beta)\omega^2 + 1 - \beta$. The roots of this quartic are $\pm\omega^+_{\mathcal{C}}, \pm\omega^-_{\mathcal{C}}$, where

$$\omega^\pm_{\mathcal{C}} = \sqrt{-1 - \frac{\beta}{2} \pm \frac{1}{2}\sqrt{\beta(\beta+8)}}. \tag{4.10}$$

All four roots exist if $\beta \le -8$ (with $\omega^+_{\mathcal{C}} = \omega^-_{\mathcal{C}}$ when $\beta = -8$), no roots exist if $-8 < \beta < 1$, and only $\pm\omega^+_{\mathcal{C}}$ exists if $\beta \ge 1$ ($\omega^+_{\mathcal{C}} = 0$ when $\beta = 1$). This yields the following ranges:

$$\begin{aligned} \beta < -8 \quad &: \quad \mathcal{C}(\omega) > 0 \quad \text{for} \quad 0 < \omega < \omega^-_{\mathcal{C}},\ \omega^+_{\mathcal{C}} < \omega, \\ &\quad\ \ \mathcal{C}(\omega) < 0 \quad \text{for} \quad \omega^-_{\mathcal{C}} < \omega < \omega^+_{\mathcal{C}}, \\ -8 \le \beta \le 1 \quad &: \quad \mathcal{C}(\omega) > 0 \quad \text{for} \quad 0 < \omega, \omega \ne \omega^\pm_{\mathcal{C}}, \\ 1 < \beta \quad &: \quad \mathcal{C}(\omega) < 0 \quad \text{for} \quad 0 < \omega < \omega^+_{\mathcal{C}}, \\ &\quad\ \ \mathcal{C}(\omega) > 0 \quad \text{for} \quad \omega^+_{\mathcal{C}} < \omega. \end{aligned}$$

Now consider the case $d < 0$. The characteristic equation factors as

$$\begin{aligned} &\Delta^-_+(\lambda)\Delta^-_-(\lambda) \\ &\quad \equiv \left[(1+\lambda)^3 - \beta + i(1+\lambda)^2\sqrt{-d}e^{-\tau\lambda}\right]\left[(1+\lambda)^3 - \beta - i(1+\lambda)^2\sqrt{-d}e^{-\tau\lambda}\right] = 0. \end{aligned} \tag{4.11}$$

Clearly, neither factor has a zero root. Note that λ is a root of $\Delta^-_+(\lambda)$ iff $\bar{\lambda}$ is a root of $\Delta^-_-(\lambda)$. This is a consequence of the fact that the roots of the unfactored characteristic equation (4.4) come in complex conjugate pairs. Following a similar procedure to that for $d > 0$, pure imaginary roots $i\omega, -i\omega$ with $\omega > 0$, of the first and second factors, respectively, exist along the curves $(d, \tau) = (-d_{im}(\omega), \tau^-_{k+}(\omega))$. Similarly, pure imaginary roots $-i\omega, i\omega$ with $\omega > 0$, of the first and second factors,

respectively, exist along the curves $(d,\tau)=(-d_{im}(\omega),\tau^-_{k\,-}(\omega))$. Here

$$\tau^-_{k\,+}(\omega)\equiv\frac{1}{\omega}\begin{cases}\operatorname{Arctan}\left(\frac{\mathcal{C}(\omega)}{\mathcal{S}(\omega)}\right)+2k\pi, & \mathcal{S}(\omega)<0,\\ \operatorname{Arctan}\left(\frac{\mathcal{C}(\omega)}{\mathcal{S}(\omega)}\right)+(2k+1)\pi, & \mathcal{S}(\omega)>0,\end{cases}\tag{4.12}$$

$$\tau^-_{k\,-}(\omega)\equiv\frac{1}{\omega}\begin{cases}\operatorname{Arctan}\left(\frac{\mathcal{C}(\omega)}{\mathcal{S}(\omega)}\right)+2k\pi, & \mathcal{S}(\omega)>0,\\ \operatorname{Arctan}\left(\frac{\mathcal{C}(\omega)}{\mathcal{S}(\omega)}\right)+(2k+1)\pi, & \mathcal{S}(\omega)<0.\end{cases}\tag{4.13}$$

The zeros of $\mathcal{S}(\omega)$ define the points where the branches join. To make the definitions of $\tau^-_{k\pm}$ more precise, the sign of $\mathcal{S}(\omega)$ with $\omega_{\mathcal{S}}=\sqrt{\sqrt{-2\beta}-1}$ is given as follows:

$$\begin{array}{rcll}\beta<-\frac{1}{2} & : & \mathcal{S}(\omega)<0 & \text{for}\quad 0<\omega<\omega_{\mathcal{S}},\\ & & \mathcal{S}(\omega)>0 & \text{for}\quad \omega_{\mathcal{S}}<\omega,\\ \beta\geq-\frac{1}{2} & : & \mathcal{S}(\omega)>0 & \text{for}\quad 0<\omega.\end{array}$$

To determine what these curves look like, we use the following results that are derived by using L'Hôpital's rule. Note that we consider only $\tau\geq 0$.

LEMMA 4.2. *For the functions in* (4.7)–(4.9), (4.12), (4.13),

$$d_{im}(0)=d_0,\ \lim_{\omega\to\infty}d_{im}(\omega)=\infty;\ \lim_{\omega\to\infty}\tau^{\pm}_{k\,\pm}=0;$$

$$\lim_{\omega\to0^+}\tau^+_{k\,\pm}=\infty,\ k>0;\quad \lim_{\omega\to0^+}\tau^+_{0\,+}=\begin{cases}2+\frac{3}{\beta-1}, & \beta>1,\\ \infty, & \beta\leq1;\end{cases}$$

$$\lim_{\omega\to0^+}\tau^+_{0\,-}=\begin{cases}\infty, & \beta>1,\\ -\infty, & \beta=1,\\ 2+\frac{3}{\beta-1}, & \beta<1;\end{cases}$$

$$\lim_{\omega\to0^+}\tau^-_{k\,\pm}=\infty,\ k>0;\quad \lim_{\omega\to0^+}\tau^-_{0\,+}=\begin{cases}-\infty, & \beta<-\frac{1}{2},\\ \infty, & \beta\geq-\frac{1}{2};\end{cases}$$

$$\lim_{\omega\to0^+}\tau^-_{0\,-}=\begin{cases}\infty, & \beta<1,\\ 1, & \beta=1,\\ -\infty, & \beta>1.\end{cases}$$

LEMMA 4.3. *For* $\frac{1}{2}(5-3\sqrt{3})\leq\beta\leq12-4\sqrt{5}$, *i.e.,* β *approximately* $\in[-0.0981, 3.0557]$, $d_{im}(\omega)$ *is a nondecreasing function of* ω. *Outside this interval it is nonmonotone and has the following behavior. For* $\beta<\frac{1}{2}(5-3\sqrt{3})$ *or* $\beta\geq\frac{1}{2}(5+3\sqrt{3})\approx5.0981$, *there exists* $\omega_c>0$ *such that* $d_{im}(\omega)$ *is decreasing for* $0<\omega<\omega_c$ *and increasing for* $\omega>\omega_c$. *For* $12-4\sqrt{5}<\beta<\frac{1}{2}(5+3\sqrt{3})$, *there exist* $0<\omega_{c1}<\omega_{c2}$ *such that* $d_{im}(\omega)$ *is increasing for* $0<\omega<\omega_{c1}$ *and* $\omega>\omega_{c2}$ *and decreasing for* $\omega_{c1}<\omega<\omega_{c2}$.

Proof. From (4.7) it is clear that

$$\frac{d\,d_{im}}{d\omega}=2\omega\frac{\omega^6+3\omega^4+3(1-2\beta)\omega^2+2\beta(5-\beta)+1}{(1+\omega^2)^3};\tag{4.14}$$

thus the sign of $\frac{d\,d_{im}}{d\omega}$ is determined by $\Omega^3+3\Omega^2+3(1-2\beta)\Omega+2\beta(5-\beta)+1$, where $\Omega=\omega^2$. Consideration of the sign of the constant term shows that the cubic has an

even number of positive roots if $\beta \in [\frac{1}{2}(5-3\sqrt{3}), \frac{1}{2}(5+3\sqrt{3}))$ and an odd number otherwise. The discriminant of this cubic is a positive multiple of $-\beta^2(\beta^2-24\beta+64)$, which is nonnegative for $\beta \in [12-4\sqrt{5}, 12+4\sqrt{5}]$ and negative otherwise. Thus outside this interval the cubic has one real root, and inside it has three. For $\beta \in [\frac{1}{2}(5-3\sqrt{3}), 12-4\sqrt{5})$, the cubic has no positive roots and at $\beta = 12-4\sqrt{5}$ it has a double positive root. Consideration of the graph of the cubic in Ω shows that $\frac{d\,d_{im}}{d\omega} \geq 0$ for $\beta \in [\frac{1}{2}(5-3\sqrt{3}), 12-4\sqrt{5}]$, and hence $d_{im}(\omega)$ is a nondecreasing function of ω. For $\beta < \frac{1}{2}(5-3\sqrt{3})$ or $\beta \geq \frac{1}{2}(5+3\sqrt{3})$ the cubic has one positive root, Ω_c. Let $\omega_c = \sqrt{\Omega_c}$. For $12-4\sqrt{5} < \beta < \frac{1}{2}(5+3\sqrt{3})$, the cubic has two positive roots $\Omega_{c1} < \Omega_{c2}$. Let $\omega_{cj} = \sqrt{\Omega_{cj}}$. The results follow from the graph of the cubic. ∎

LEMMA 4.4. *For fixed β, τ, the number of roots of* (4.4) *with positive real part increases (decreases) by two as τ increases through one of the curves $(d,\tau) = (d_{im}, \tau^+_{k\pm})$, where d_{im} is an increasing (decreasing) function of ω. The number of roots of* (4.4) *with positive real part increases (decreases) by two as τ increases through one of the curves $(d,\tau) = (-d_{im}, \tau^-_{k\pm})$, where $-d_{im}$ is a decreasing (increasing) function of ω.*

Proof. Consider the first factor of (4.5). Differentiating with respect to τ gives

$$\frac{d\lambda}{d\tau} = \frac{\lambda(1+\lambda)\sqrt{d}e^{-\tau\lambda}}{3(1+\lambda)+\sqrt{d}e^{-\tau\lambda}(2-\tau(1+\lambda))}.$$

Using (4.5) to eliminate $e^{-\tau\lambda}$ and setting $\lambda = i\omega$ yield

$$\left.\frac{d\lambda}{d\tau}\right|_{\lambda=i\omega} = \frac{i\omega\left[\beta+4\omega^2-(1-\omega^2)^2+i\omega(\beta-4(1-\omega^2))\right]}{1-3\omega^2+2\beta-\tau(\beta+4\omega^2-(1-\omega^2)^2)+i\omega[3-\omega^2-\tau(\beta-4(1-\omega^2))]}.$$

Taking the real part gives

$$\left.\frac{d\,[\mathrm{Re}(\lambda)]}{d\tau}\right|_{\lambda=i\omega} = \frac{\omega^2}{K_1^2+K_2^2}\left(\omega^6+3\omega^4+3(1-2\beta)\omega^2+2\beta(5-\beta)+1\right),$$

where

$$K_1 = 1-3\omega^2+2\beta-\tau(\beta+4\omega^2-(1-\omega^2)^2), \qquad K_2 = \omega[3-\omega^2-\tau(\beta-4(1-\omega^2))].$$

The second factor of (4.5) or either factor of (4.11) yields the same expression. Using (4.14) gives

$$\left.\frac{d\,[\mathrm{Re}(\lambda)]}{d\tau}\right|_{\lambda=i\omega} = \frac{\omega(1+\omega^2)^3}{2(K_1^2+K_2^2)}\,\frac{d\,d_{im}}{d\omega},$$

along the curves associated with pure imaginary roots of (4.5). Along the curves associated with pure imaginary roots of (4.11), d_{im} is replaced by $-d_{im}$ so the derivative is of opposite sign. The result follows. ∎

From section 3, when $\tau = 0$ and $\beta < -\frac{1}{2}$ the characteristic equation has a pair of pure imaginary roots $\lambda = \pm i\sqrt{-1+\sqrt{-2\beta}} = \pm i\omega_{\mathcal{S}}$ at the positive value $d = d^+ \equiv (2-\sqrt{-\beta/2})^2$. Similarly, when $\tau = 0$ and $\beta \leq -8$ the characteristic equation has pairs of pure imaginary roots $\lambda = \pm i\omega_{\mathcal{C}}^+, \pm i\omega_{\mathcal{C}}^-$, as defined in (4.10), at the following negative values of d:

$$d^-_{\pm} \equiv -\frac{\omega_{\mathcal{C}}^{\pm\,2}(\omega_{\mathcal{C}}^{\pm\,2}-3)^2}{(1-\omega_{\mathcal{C}}^{\pm\,2})^2}.$$

The roots at d_+^- also occur when $\beta > 1$. Note that d^+ must correspond to the value of d_{im} when $\tau = 0$ and $d_\pm^-$ to values of $-d_{im}$ when $\tau = 0$. More specifically, the definitions (4.8)–(4.9) and (4.12)–(4.13) of $\tau_{k\pm}^{\pm}$ give the following. For $\beta \le -8$, d^+ is the d intercept of the curve $(d_{im}(\omega), \tau_{0+}^{+}(\omega))$ and $d_\mp^-$ are the d intercepts of the curves $(-d_{im}(\omega), \tau_{0\pm}^{-}(\omega))$. For $-8 < \beta < -\frac{1}{2}$, d^+ is the d intercept of the curve $(d_{im}(\omega), \tau_{0-}^{+}(\omega))$. For $\beta > 1$, d_+^- is the d intercept of the curve $(-d_{im}(\omega), \tau_{0-}^{-}(\omega))$.

We now describe the region of stability of the trivial equilibrium in the $d\tau$-plane for intervals of values of β by finding bifurcation curves on which an eigenvalue has zero real part. This is the content of the rest of this section. Theorem 4.5 is illustrated (using Maple) in Figure 4.1(a) with $\beta = 1.5$, Theorem 4.6 is illustrated in Figure 4.1(b) with $\beta = 0.1$, and Theorem 4.7 is illustrated in Figure 4.4 with $\beta = -10$.

THEOREM 4.5. *Let $1 \le \beta \le 12 - 4\sqrt{5}$ be fixed. Then the trivial solution of* (4.1) *is linearly asymptotically stable for $d < d_+^-$, $0 \le \tau < \tau_{0-}^{-}$.*

Proof. From section 3, for $\tau = 0$ and $\beta \ge 1$, all roots of the characteristic equation have negative real parts if $d < d_+^-$ (see Figure 3.1). For fixed β and d, as τ is increased the number of roots with positive real parts remains the same until τ reaches the smallest value for which the characteristic equation has a pair of pure imaginary roots. This value is τ_{0-}^{-}. To see this, note from Lemma 4.4 that d_{im} is a continuous nondecreasing function of ω with $0 \le d_0 \le d_{im} < \infty$ and that $d_+^- < -d_0$. Thus for any fixed $d < d_+^-$ there is one positive value of ω such that $-d_{im}(\omega) = d$. Further, it is straightforward to show that, for any value of ω, $\tau_{0-}^{-}(\omega) < \tau_{0+}^{-}(\omega) < \tau_{k\pm}^{-}(\omega)$ for $k = 1, 2, \ldots$. Thus all the roots of the characteristic equation have negative real parts in the given range of d and τ. Applying the results of Lemma 4.4 shows there is at least one root of the characteristic equation with positive real part everywhere else in the $d\tau$-plane. ∎

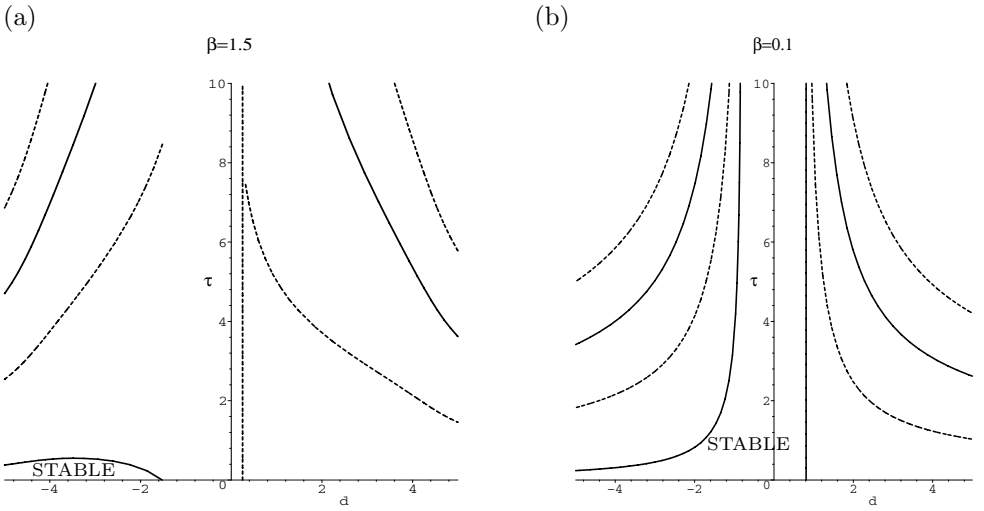

FIG. 4.1. *Bifurcation curves for the trivial solution of* (4.1) *for* (a) $\beta = 1.5$, (b) $\beta = 0.1$. *The stability region is qualitatively the same for* (a) $1 \le \beta \le 12 - 4\sqrt{5}$, (b) $\frac{1}{2}(5 - 3\sqrt{3}) \le \beta < 1$. *Along the solid (dashed) curves with $d > 0$, $\Delta_-^+(\lambda)$ ($\Delta_+^+(\lambda)$) has a pair of pure imaginary roots. Along the solid (dashed) vertical line $d = d_0$, $\Delta_-^+(\lambda)$ ($\Delta_+^+(\lambda)$) has a zero root. Along the solid (dashed) curves with $d < 0$, $\Delta_-^-(\lambda)$ ($\Delta_+^-(\lambda)$) has a root $i\omega$ with $\omega > 0$ and $\Delta_+^-(\lambda)$ ($\Delta_-^-(\lambda)$) has the complex conjugate root $-i\omega$.*

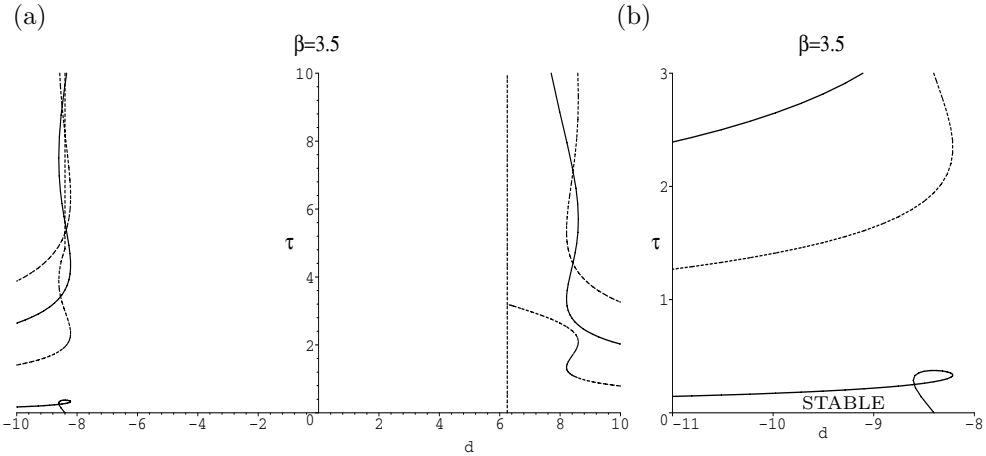

FIG. 4.2. (a) *Bifurcation curves for the trivial solution of* (4.1) *for* $\beta = 3.5$. (b) *Close-up showing stability region. The meaning of the solid and dashed curves are as described for Figure* 4.1.

THEOREM 4.6. *Let* $\frac{1}{2}(5-3\sqrt{3}) \le \beta < 1$ *be fixed. Then the trivial solution of* (4.1) *is linearly asymptotically stable for* $-d_0 \le d < d_0$, $0 \le \tau$ *or* $d < -d_0$, $0 \le \tau < \tau_{0-}^{-}$.

Proof. From section 3, for $\tau = 0$ and $\frac{1}{2}(5 - 3\sqrt{3}) \le \beta < 1$, all roots of the characteristic equation have negative real parts if $d < d_0$ (see Figure 3.1). Using the same argument as in the proof of Theorem 4.5, it can be shown that all roots of the characteristic equation have negative real parts for $d < -d_0$ and $0 \le \tau < \tau_{0-}^{-}$. From Lemma 4.3, d_{im} is a monotone function of ω for the assumed β range. Thus, using Lemma 4.2 for $\omega > 0$, $d_{im}(\omega) \ge d_{im}(0) = d_0$ and $-d_{im}(\omega) \le -d_{im}(0) = -d_0$. Hence for $-d_0 \le d < d_0$ and $\tau \ge 0$ all roots of the characteristic equation have negative real parts. The rest of the proof is the same as for Theorem 4.5. □

When β no longer lies in the first range given in Lemma 4.3, the curves along which the characteristic equation has pure imaginary roots become nonmonotone. This has two consequences. First, there will be values of ω such that $d_{im}(\omega) < d_0$, and second, there may exist intersection points of the curves $(d_{im}(\omega), \tau_{j\pm}^{+}(\omega))$ and $(-d_{im}(\omega), \tau_{j\pm}^{-}(\omega))$ with each other and with the line $d = d_0$. In this situation, the boundary of the stability region is made up of pieces of the curves $(d_{im}(\omega), \tau_{j\pm}^{+}(\omega))$ and $(-d_{im}(\omega), \tau_{j\pm}^{-}(\omega))$ and of the line $d = d_0$.

Consider first the case $\beta > 12 - 4\sqrt{5}$. For this range of β, we observe that $(d, \tau) = (-d_{im}, \tau_{0-}^{-})$ intersects itself. The stability region is still bounded by the d axis for $d < d_{+}^{-}$ and the curve $(-d_{im}(\omega), \tau_{0-}^{-}(\omega))$. However, part of the curve now forms a loop, inside which the trivial solution is unstable (this may be verified by applying Lemma 4.4). This is illustrated in Figure 4.2 with $\beta = 3.5$. We believe that the stability region is qualitatively the same for any $\beta > 12 - 4\sqrt{5}$.

Now consider the range $\beta < \frac{1}{2}(5 - 3\sqrt{3})$. For $\beta \le -\frac{1}{2}$ part of the curve of pure imaginary eigenvalues $(d_{im}(\omega), \tau_{0-}^{+}(\omega))$ enters the nonnegative τ region (this can be seen from the limits in Lemma 4.2). Using this fact, the discussion above, and the results of Lemmas 4.2 and 4.3, it can be shown that for $-\frac{1}{2} \le \beta < \frac{1}{2}(5 - 3\sqrt{3})$ the stability region looks qualitatively as depicted in Figure 4.3(a) and for $-8 < \beta < -\frac{1}{2}$ it looks qualitatively as depicted in Figure 4.3(b).

As β is decreased, the curves of pure imaginary eigenvalues approach the τ axis (and the stability region shrinks) until at $\beta = -8$ their points of minimal d value actually touch the τ axis. Recall that for $\beta < -8$, the curves $(-d_{im}(\omega), \tau_{0-}^{-}(\omega))$

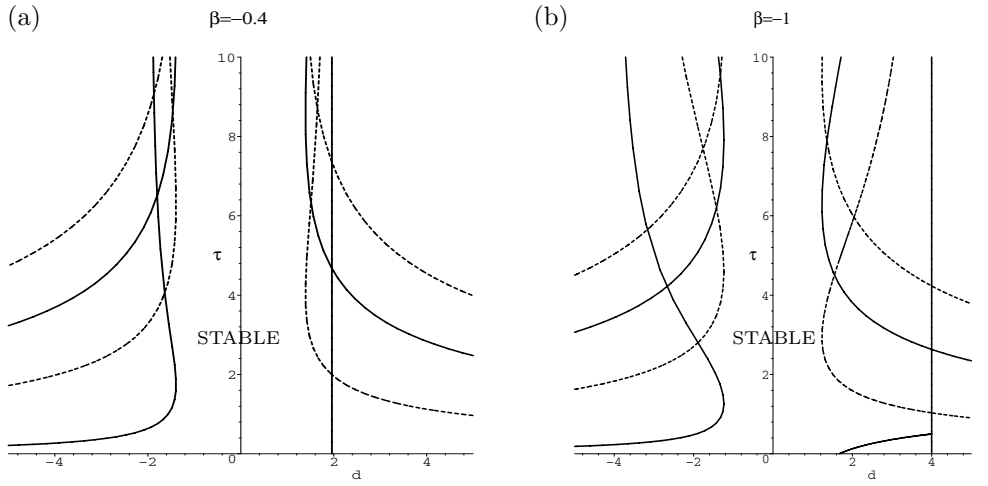

FIG. 4.3. *Bifurcation curves for the trivial solution of* (4.1) *for* (a) $\beta = -0.4$, (b) $\beta = -1$. *The stability region is qualitatively the same for* (a) $-\frac{1}{2} \le \beta < \frac{1}{2}(5 - 3\sqrt{3})$, (b) $-8 < \beta < -\frac{1}{2}$. *The meaning of the solid and dashed curves is as described for Figure* 4.1.

and $(-d_{im}(\omega), \tau_{0+}^{-}(\omega))$ intersect the d axis at d_+^- and d_-^-, respectively. From their definitions, (4.12)–(4.13), and the fact that $d_-^- < d_+^-$, these curves must have an intersection point. We denote this point by (d_{int}, τ_{int}) and have the following result, illustrated in Figure 4.4, for $\beta = -10$.

THEOREM 4.7. *Let $\beta \le -8$ be fixed. Then the trivial solution of* (4.1) *is linearly asymptotically stable for $d < d_-^-$, $0 \le \tau < \tau_{0-}^{-}$ or $d_-^- \le d < d_{int}$, $\tau_{0+}^{-} < \tau < \tau_{0-}^{-}$.*

Proof. From section 3, for $\tau = 0$ and $\beta \le -8$, all the roots of the characteristic equation have negative real parts if $d < d_-^-$ (see Figure 3.1). Using the same argument as in the proof of Theorem 4.5, it can be shown that all roots of the characteristic equation have negative real parts for $d < d_-^-$ and $0 \le \tau < \tau_{0-}^{-}$. For $\tau = 0$ and $d_-^- < d < d_+^-$, the characteristic equation has two roots with positive real parts.

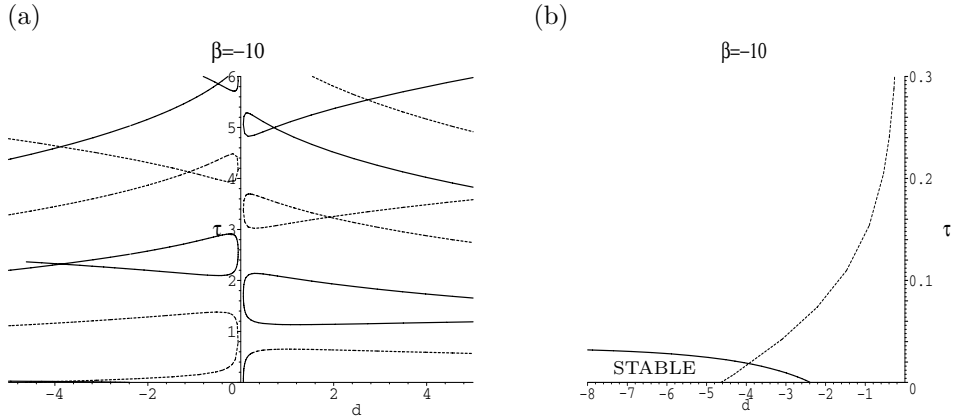

FIG. 4.4. (a) *Bifurcation curves for the trivial solution of* (4.1) *for* $\beta = -10$. (b) *Close-up showing stability region. The stability region is qualitatively the same for any* $\beta \le -8$. *The meaning of the solid and dashed curves is as described for Figure* 4.1.

Applying Lemma 4.4 shows that the number of roots with positive real parts decreases by two along the part of $(-d_{im}(\omega), \tau_{0+}^{-}(\omega))$, where $-d_{im}$ is increasing, and increases by two along the part of $\left(-d_{im}(\omega), \tau_{0-}^{-}(\omega)\right)$, where $-d_{im}$ is decreasing. The rest of the proof is the same as for Theorem 4.5. □

4.2. Bifurcations. In the previous subsection, we determined all points in parameter space where the trivial solution of (4.2) has eigenvalues with zero real parts. The bifurcations that may occur at such points as a system parameter is varied are important, particularly when they lie on the boundary of the stability region, as they determine the observable behavior of the system.

Consider first the case when a zero root of (4.4) exists. This occurs for parameter values along the line $d = d_0$. For $\beta \neq 1$, it can be shown that the conditions for a pitchfork bifurcation to occur are satisfied at almost all points on this line. In particular, taking d as the bifurcation parameter, Lemma 4.1 shows that the root is simple for $\beta \neq 1$ and $\tau \neq 2 + \frac{3}{\beta - 1}$. To ensure that the characteristic equation has no other roots with zero real part, the points of intersection of the line $d = d_0$ with the curves $(d_{im}(\omega), \tau_{\pm}^{+}(\omega))$ and $(-d_{im}(\omega), \tau_{\pm}^{-}(\omega))$ must also be excluded. In terms of the original model parameters, taking d as the bifurcation parameter is equivalent to fixing b, τ, and one of the c_j and using the other c_j as the bifurcation parameter.

Consider now the case when a pair of pure imaginary roots of (4.4) exists. This occurs for parameter values on the curves $(d_{im}(\omega), \tau_{\pm}^{+}(\omega))$ and $(-d_{im}(\omega), \tau_{\pm}^{-}(\omega))$. A statement of the Hopf bifurcation theorem for delay equations can be found in [12, Chapter 11]. It can be shown that this theorem is satisfied at almost all points on these curves. In particular, taking τ as the bifurcation parameter, Lemma 4.4 shows that the roots are simple at all points where $\frac{dd_{im}}{d\omega} \neq 0$. To ensure that the characteristic equation has no other roots with zero real part, the points of intersection of each curve with $d = d_0$ and the other curves where pure imaginary roots exist must be excluded.

If there is slightly more symmetry in the model, then some interesting patterns in the bifurcating solutions emerge. Suppose that $c_1 = c_2 = c$, as in parts of section 3 (e.g., Theorem 3.2), implying that $d = b^2c^2 > 0$. In this case, only the pitchfork bifurcation and the Hopf bifurcations along $(d_{im}(\omega), \tau_{\pm}^{+}(\omega))$ can occur. Consider the bifurcations that occur at a point in parameter space where $\Delta_{-}^{+}(\lambda)$ has a root with zero real part. (This corresponds to the solid curves in the figures of the previous subsection.) When $bc > 0$ it is straightforward to show that the solution of (4.2) corresponding to a root λ of $\Delta_{-}^{+}(\lambda)$ has the form $e^{\lambda t}(y_1, y_2, y_3, y_1, y_2, y_3)^t$. Thus we expect that the bifurcating solutions have a similar property—namely, the corresponding elements of the two loops are in phase, or synchronized. Similarly, when $bc < 0$ the solution of (4.2) corresponding to a root λ of $\Delta_{-}^{+}(\lambda)$ has the form $e^{\lambda t}(y_1, y_2, y_3, -y_1, -y_2, -y_3)^t$, and we expect the bifurcating solutions have corresponding elements of the two loops antiphase (or half a period out of phase). The solutions corresponding to roots of $\Delta_{+}^{+}(\lambda)$ have just the opposite property. When $bc > 0$ they are antiphase and when $bc < 0$ they are in-phase. When $c_1 \neq c_2$ but $c_1 \approx c_2$, we expect that bifurcating solutions are almost in-phase or almost antiphase. Such behavior was observed in [18].

Now suppose that $c_1 = -c_2 = c$, implying that $d = -b^2c^2 < 0$. In this case, only Hopf bifurcations along the curves $(-d_{im}(\omega), \tau_{\pm}^{-}(\omega))$ occur. When the characteristic equation has a pair of roots $\lambda = \pm i\omega$, corresponding solutions of (4.2) have the form $e^{\lambda t}(y_1, y_2, y_3, \pm iy_1, \pm iy_2, \pm iy_3)^t$. Thus corresponding elements of the bifurcating periodic orbits are one quarter period out of phase. When $c_1 \neq -c_2$ but $c_1 \approx -c_2$,

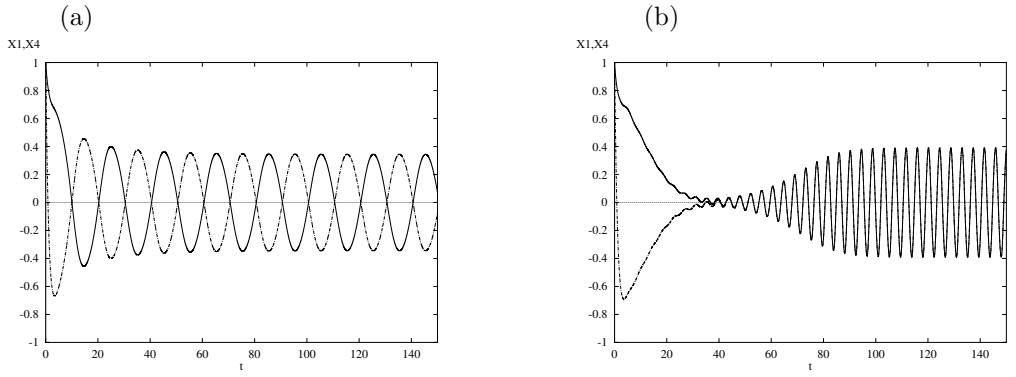

FIG. 4.5. *Numerical simulations of* (4.1) *with* $b = -1$, $c_1 = c_2 = 1.75$. *The plots in each case show* x_1 *(solid line) and* x_4 *(dot-dash line) vs.* t. (a) $\tau = 0.3$*; periodic orbit with* $x_4(t) = -x_1(t)$. (b) $\tau = 1.5$*; periodic orbit with* $x_4(t) = x_1(t)$. *Initial conditions for both cases* $x(t) = (1, -0.7, -0.9, 1.1, 0.8, 1.2)^t$, $-\tau \le t \le 0$.

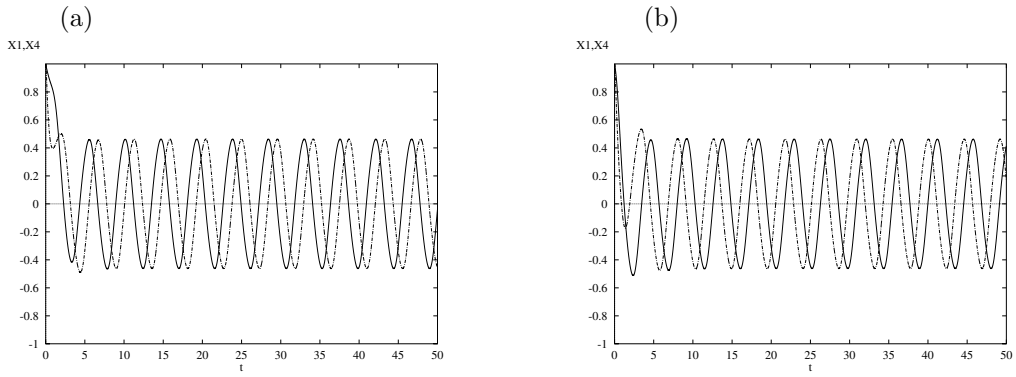

FIG. 4.6. *Numerical simulations of* (4.1) *with* $b = -1$, $\tau = 0.5$, *and* $c_1 = -c_2$. *The plots in each case show* x_1 *(solid line) and* x_4 *(dot-dash line) vs.* t. (a) $c_1 = 1.75$*; periodic orbit with* $x_4(t) = x_1(t - \frac{T}{4})$, *where* T *is the period.* (b) $c_1 = -1.75$*; periodic orbit with* $x_4(t) = x_1(t + \frac{T}{4})$. *Initial conditions as for Figure* 4.5.

we expect that bifurcating solutions are close to one quarter period out of phase.

These results are illustrated in Figures 4.5–4.6, showing numerical simulations of (4.1), with $b = -1$ and other parameters as indicated, which correspond to points in the stability diagram of Figure 4.3(b). Only x_1 and x_4 are shown in Figures 4.5–4.6; solutions for other pairs are similar. Simulations were performed in XPPAUT [6] using a fourth order Runge–Kutta integrator adapted for delay differential equations.

5. Discussion. Combining local and global results with numerical evidence, we arrive at the following summary of the dynamics of these loops. Results are given in terms of $\beta = b^3$ and $d = b^2 c_1 c_2$, where b is the gain of the response function for each neuron and c_i are the coupling strengths between the 3-loops. The loops are inherently (i.e., in isolation) oscillatory for $\beta < -8$. The origin is proved to be globally stable for $\beta \in (-2\sqrt{2}, 1)$, and numerical evidence extends this to $(-8, 1)$. For

$\beta > 1$ the solutions approach a nontrivial stable fixed point (the origin is unstable).

The effect of coupling depends on whether it is symmetric (excitatory in both directions or inhibitory in both directions) or asymmetric (excitatory in one direction and inhibitory in the other). It is interesting that the linear stability analysis is identical for excitatory and inhibitory coupling, as long as it is the same in both directions, as it depends essentially on the product of the two coupling coefficients. This was also noted in the somewhat similar situation studied by Shayer and Campbell [18]. Symmetric coupling of sufficient strength (not necessarily very strong) can destabilize the origin in the middle (inherently stable) β range. When $\beta \in (-\frac{1}{2}, 1)$, the system goes to nontrivial fixed points, but when $\beta \in (-8, -\frac{1}{2})$, it first goes to oscillation as coupling is increased. Asymmetric coupling of sufficient strength (and here it needs to be quite strong) can stabilize the origin in either of the two inherently unstable ranges. The further β is from the inherently stable range, the stronger the coupling needs to be to accomplish this stabilization. In the case of symmetric coupling, nontrivial equilibria exist when β is large enough, but there are no nontrivial equilibria for smaller β when the coupling is weak. In the case of asymmetric coupling, there are no nontrivial equilibria for $\beta < 1$. It is not clear whether nontrivial equilibria occur for other regions of parameter space. For most regions, oscillation of the system is suggested when the linear results show that the origin is unstable.

We have observed five main delay-related phenomena in this system.

1. When coupling is asymmetric ($d < 0$) and large, the stability of the origin is weak in the sense that only a small delay is needed to destabilize it and produce oscillation. This is delay-induced oscillation or delay-induced instability, which has commonly been observed in delayed networks since the early work of Marcus and Westervelt [15].
2. In the inherently stable range $\beta \in (-8, 1)$, delay independent stability exists for weak enough coupling ($|d|$ small) whether symmetric or asymmetric.
3. For intermediate values of $|d|$ and $\beta \in (-8, -0.098)$, whether the system oscillates or settles at the origin depends on the delay in a complex way. For some delay ranges, the origin is stable, and for others it is unstable, and there can be stability/instability switches as the delay increases.
4. For $\beta \in (-8, -\frac{1}{2})$, if coupling is symmetric and fairly strong ($d > 0$ and large but still $< (1-\beta)^2$), in the region where coupling has destabilized the origin to create oscillation, there is an intermediate range of delays (not including zero but not too large) that stabilizes the origin again and suppresses the oscillations. This is delay-induced stability or *oscillator death*.
5. For equal and symmetric coupling strengths, oscillatory solutions in the two loops bifurcating from the origin may be in phase or antiphase depending on the value of the delay. For asymmetric coupling with equal strengths, corresponding neurons in the two loops oscillate one quarter period out of phase.

Some of these results are similar to those found by Shayer and Campbell [18] for a simpler coupled system. However, their work focused on the symmetric coupling case.

Some properties of coupled systems that can each potentially oscillate begin to emerge from these studies—in particular, the ways in which oscillation or instability depends on the interaction between coupling strength and coupling delay. Although the system studied here is too simple to draw definite conclusions about physiological systems, results do show that complicated effects can occur even in the simplest

coupled loops with delay. This study could be extended by investigating other patterns of coupling between two loops, such as "lateral" coupling between each corresponding pair of units in the two loops (if the loops have the same structure), or "forward" coupling as studied without delays by Edwards and Gill [5]. For applications in which the units are far apart, it would be worthwhile to include delays in connections within each loop.

Acknowledgment. We wish to acknowledge the assistance of Daisuke Shinki in carefully checking the results and proofreading the paper.

REFERENCES

[1] P. Baldi and A. Atiya, *How delays affect neural dynamics and learning*, IEEE Trans. Neural Networks, 5 (1994), pp. 612–621.

[2] H. Bergman, A. Feingold, A. Nini, A. Raz, H. Slovin, M. Abeles, and E. Vaadia, *Physiological aspects of information processing in the basal ganglia of normal and Parkinsonian primates*, Trends Neurosci., 21 (1998), pp. 32–38.

[3] S. A. Campbell, *Stability and bifurcation of a simple neural network with multiple time delays*, Fields Inst. Commun., 21 (1999), pp. 65–79.

[4] S. A. Campbell, *Delay independent stability for additive neural networks*, Differential Equations Dynam. Systems, 9 (2001) pp. 115–138.

[5] R. Edwards and P. Gill, *On synchronization and cross-talk in parallel networks*, Dyn. Contin. Discrete Impuls. Syst. Ser. B Appl. Algorithms, 10 (2003), pp. 287–300.

[6] B. Ermentrout, *Simulating, Analyzing, and Animating Dynamical Systems: A Guide to XPPAUT for Researchers and Students*, Software Environ. Tools 14, SIAM, Philadelphia, 2002.

[7] L. Glass and C. P. Malta, *Chaos in multi-looped negative feedback systems*, J. Theor. Biol., 145 (1990), pp. 217–223.

[8] L. Glass and J. S. Pasternack, *Stable oscillations in mathematical models of biological control systems*, J. Math. Biol., 6 (1978), pp. 207–223.

[9] K. Gopalsamy and X.-Z. He, *Delay independent stability in bidirectional associative memory networks*, IEEE Trans. Neural Networks, 5 (1994), pp. 998–1002.

[10] A. M. Graybiel, *Basal ganglia—input, neural activity, and relation to the cortex*, Curr. Opin. Neurobiol., 1 (1991), pp. 644–651.

[11] J. Guckenheimer and P. Holmes, *Nonlinear Oscillations, Dynamical Systems, and Bifurcations of Vector Fields*, Springer-Verlag, New York, 1983.

[12] J. Hale and S. M. V. Lunel, *Introduction to Functional Differential Equations*, Springer-Verlag, New York, 1993.

[13] N. Kopell and G. B. Ermentrout, *Phase transitions and other phenomena in chains of coupled oscillators*, SIAM J. Appl. Math., 50 (1990), pp. 1014–1052.

[14] L. Olien and J. Bélair, *Bifurcations, stability, and monotonicity properties of a delayed neural network model*, Phys. D, 102 (1997), pp. 349–363.

[15] C. Marcus and R. Westervelt, *Stability of analog neural networks with delay*, Phys. Rev. A (3), 39 (1989), pp. 347–359.

[16] I. Ncube, S. A. Campbell, and J. Wu, *Change in criticality of synchronous Hopf bifurcation in a multiple-delayed neural system*, Fields Inst. Commun., 36 (2003), pp. 179–193.

[17] K. Pakdaman, C. Grotta-Ragazzo, C. P. Malta, O. Arino, and J.-F. Vibert, *Effect of delay on the boundary of the basin of attraction in a system of two neurons*, Neural Networks, 11 (1998), pp. 509–519.

[18] L. P. Shayer and S. A. Campbell, *Stability, bifurcation, and multistability in a system of two coupled neurons with multiple time delays*, SIAM J. Appl. Math., 61 (2000), pp. 673–700.

[19] P. van den Driessche, J. Wu, and X. Zou, *Stabilization role of inhibitory self-connections in a delayed neural network*, Phys. D, 150 (2001), pp. 84–90.

[20] P. van den Driessche and X. Zou, *Global attractivity in delayed Hopfield neural network models*, SIAM J. Appl. Math., 58 (1998), pp. 1878–1890.

[21] J. Wu, T. Faria, and Y. S. Huang, *Synchronization and stable phase-locking in a network of neurons with memory*, Math. Comput. Modelling, 30 (1999), pp. 117–138.